

## Method Controlling Two or More Sets of PMSM by One Inverter on a Railway Vehicle

Takuma Ito<sup>\*</sup>, Hiromi Inaba<sup>\*</sup>, Keiji Kishine<sup>\*</sup>, Mitsuki Nakai<sup>\*\*</sup> and Keisuke Ishikura<sup>\*</sup>

**Abstract** – If two or more Permanent Magnet Synchronous Motors (PMSM) can be controlled by one inverter, a train can be driven by less energy than the present Induction Motor (IM) drive system. First, this paper proposes a method for simulating the movement of wheels and a vehicle to develop a control method. Next, a method is presented for controlling two or more PMSMs by one inverter.

**Keywords:** Multi Motor Drive, Railway Vehicle, Synchronous Machine

### 1. Introduction

Trains are now being driven by mainly operating two or more induction motors by one inverter. However, trains could be made more efficient by using a permanent magnet synchronous motor (PMSM) instead of an induction motor. Fig. 1 shows a railway vehicle model that can be run by plural PMSMs and one inverter. This paper proposes a method for simulating movement of wheels and a vehicle for an electricity system package program (PSIM) and a control method in which one inverter is used to control two or more PMSMs that have different magnetic pole positions.

### 2. Modeling of Driving Part

Fig. 2 shows a wheel movement simulation model. The wheel sits on the disk (called a rail disk) equivalent to an endless rail, and the disk is rotated by friction between the wheel and the disk. The wheel is joined to the axis of the PMSM. (In practice, in the structure of a railway vehicle, motor power is transmitted to wheel through reduction gears. However, it is transmitted directly in this simulation.) Fig. 2 explains the of motion caused by the side of a wheel and a rail disk. The positive rotation direction is defined as the direction of the arrow in Fig. 2. (1) shows the of motion for a wheel.  $J_r$  is the moment of inertia of a wheel.

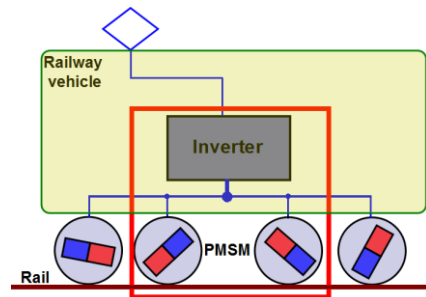


**Fig. 1.** Vehicle model to be controlled by plural PMSM and single inverter

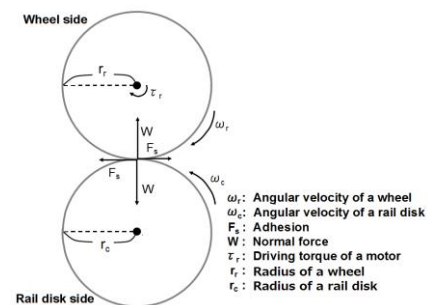


**Fig. 2.** Wheel movement simulation model

$$J_r \frac{d\omega_r}{dt} = \tau_r - \tau_s \quad (1)$$

(2) shows the of motion for a rail disk.  $J_c$  is the moment of inertia of a rail disk.

$$J_c \frac{d\omega_c}{dt} = \tau_s - \tau_c \quad (2)$$

The power  $F_s$  committed between a wheel and a rail disk is explained.  $F_s$  is a power called the adhesion, which arises at the contact point of a wheel and a disk. (3) shows the

<sup>\*</sup> Dept. of Electrical Systems Engineering, the University of Shiga Prefecture, Japan. (zn23titou@ec.usp.ac.jp, inaba.h@usp.ac.jp, kishine.k@usp.ac.jp, zn23kishikura@ec.usp.ac.jp)

<sup>\*\*</sup> Ishida Co., Ltd., Japan. (mimimi.mitsuki@gmail.com)

formula that calculates  $F_s$ .  $\mu$  is the adhesion coefficient, and  $W$  is the normal reaction.

$$F_s = \mu W \quad (3)$$

If the wheel is faster than the rail disk, the adhesion coefficient  $\mu$  is a value determined by the slip ratio  $s$  of the rail disk speed and wheel speed.

(4) shows the formula that calculates slip ratio  $s$ .

$$s = \frac{\omega_r r_r - \omega_c r_c}{\omega_r r_r} \quad (4)$$

Fig. 3 shows a general relationship between the adhesion coefficient  $\mu$  and slip ratio  $s$  [1]. The value of slip ratio  $s$  is less than 1% where the adhesion coefficient  $\mu$  maximizes. The adhesion hinders rotation of a wheel, but it rotates a rail disk. The simulation method for movement of wheels and a vehicle is described. (5) shows the fundamental of rotational motion.  $J$  expresses the moment of inertia,  $\omega$  expresses rotary speed, and  $\tau$  expresses torque.

$$J \frac{d\omega}{dt} = \tau \quad (5)$$

(6) shows the fundamental electrical of a capacitor circuit.  $C$  expresses capacitance,  $V$  expresses a voltage, and  $I$  expresses an electric current.

$$C \frac{dV}{dt} = I \quad (6)$$

[Mechanical-Electrical interface block] can be used in PSIM, which makes it possible to think the electric (6) is equivalent to the mechanical (5). By this interface, the equivalent circuit of the exercise can be made electrically on PSIM. Therefore, the wheel movement is simulated on the simulator by simulating the circuit of motion of the wheel movement. The following description explains that a capacitance  $C$ , an inertia moment  $J$ , a voltage  $V$  applied to  $C$ , are equivalent to a rotation speed  $\omega$ , a current  $I$ , and a torque  $\tau$ , respectively. (7) shows the electric that is equivalent to (1).

$$C_r \frac{dV_r}{dt} = I_r - I_s \quad (7)$$

(8) shows the electric that is equivalent to (2).

$$C_c \frac{dV_c}{dt} = I_s - I_c \quad (8)$$

Fig. 4(a) and (b) show equivalent circuits of (7) and (8). As shown in Fig. 4, the wheel movement was simulated on the simulator by simulating the circuit of motion of the wheel movement. For a simulation method for the adhesion, Fig. 5 shows a circuit outputting the adhesion.  $\omega_c$  and  $\omega_r$  in Fig. 5 represent angular velocity of a rail disk  $\omega_c$  and angular velocity of the wheel  $\omega_r$ . To operate the circuit in Fig. 5, first rate  $s$  from (4) is calculated using angular velocity. Next, the adhe

sion coefficient  $\mu$  is calculated from the

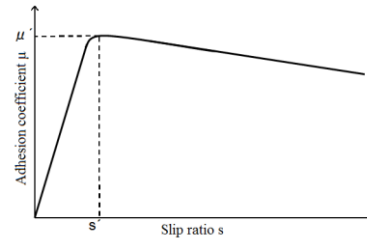
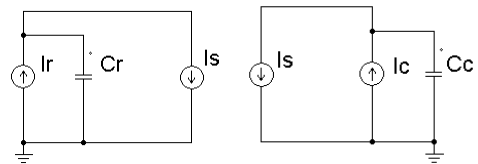


Fig. 3. Relationship between adhesion coefficient  $\mu$  and slip ratio  $s$



(a) Case of (7) (b) Case of (8)

Fig. 4. Equivalent circuits of (7) and (8)

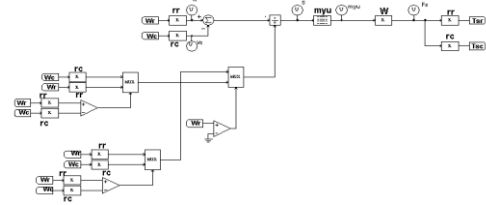


Fig. 5. Circuit of outputting the adhesion

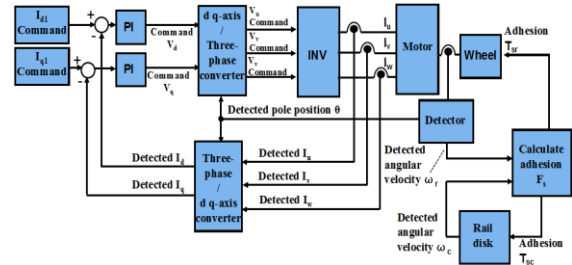


Fig. 6. Block diagram of wheel motion simulation for one wheel

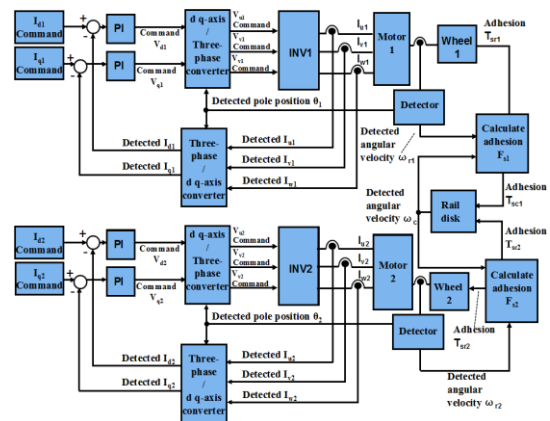


Fig. 7. Block diagram of wheel motion simulation for two wheels

calculated slip ratio  $s$ . Myu in Figure 5 represents the function block, and it outputs the adhesion coefficient  $\mu$  corresponding to that in Fig. 3 by inputting the value of the calculated slip rate  $s$ .

Thereafter, the adhesion  $F_s$  is calculated from (3). Next, the adhesion torque  $T_{sr}$  and  $T_{sc}$  is calculated from the radius of the disk. Finally, the value of calculated adhesion torque is outputted to the circuit as current source  $I_{sr}$  and  $I_{sc}$ .

Fig. 6 shows a block diagram of wheel motion simulation for one wheel. Vector control is used to control PMSM. Also, if two or more wheels ride on the rail, they are simulated as well. Fig. 7 shows a block diagram of wheel motion simulation for two wheels. Two inverters control the PMPM, and the adhesion arises between each of the rails and wheels.

### 3. Consideration of Control Method

Fig. 8 shows the model of two PMSMs in which the magnetic pole position differs and one inverter. If PMSM is controlled using the vector control, PMSM is controlled on the dq-axis coordinates that are calculated by the detected magnetic pole position. When two PMSMs that have different magnetic pole positions are driven by a single inverter, if the vector is controlled in accordance with the magnetic pole position of one side of PMSM, the other side of PMSM is controlled by an angle that deviates from the actual position of the magnetic pole. For the other side of PMSM, when PMSM is controlled by an angle that deviates from the actual position of the magnetic pole, considering how the deviation affects the output torque. Evaluation is carried out by giving an error of an angle  $X$  to the angle  $\theta$  that is actually detected. Fig. 9 shows a block diagram of granting a magnetic pole position error  $X$ . In this case, vector control is performed in one PMSM by the error detection angle  $\theta' (= \theta + X)$  using one inverter. Simulating in Fig9 in the case that giving the detected angle error  $X = [0,10,20,30, \dots ,360]$ . Measuring the output torque  $\tau_R$  and q-axis current  $I_q$  in this simulate.

Fig. 10 shows the relationship between the output torque  $\tau$  and the detection error angle  $X$ . The vertical axis in Fig. 10 shows the percentage of the output torque to the current when the percentage is defined as 100% at  $X = 0$ . In Fig. 10, the relationship between detection angle error  $X$  and output torque  $\tau$  becomes  $\tau = \cos X$ . The relationship between the output torque and the detection error  $X$  became  $\cos$  waveform. For this reason, the output torque is determined by the size of  $I_q$ . However, the q-axis current  $I_q$  of the detection error direction is controlled in a direction shifted  $\theta$  from the no error direction. Therefore, it is considered that

real  $I_q$  becomes a value that is multiplied by  $\cos\theta$  to the  $I_q$  of the detection error direction. Therefore, the decrease in output torque is acceptable to some extent if there is detection error  $X$  in the range of around  $\pm 20$  degrees. However, further error is hard to permit.

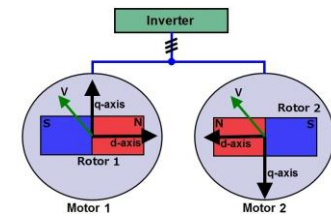


Fig. 8. Model of two PMSMs

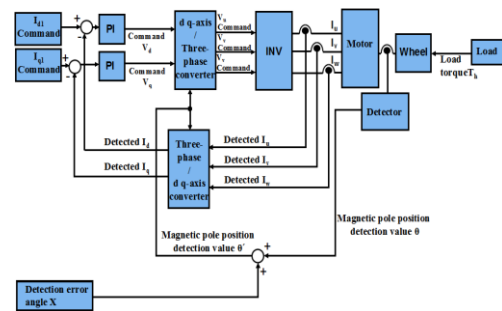


Fig. 9. Block diagram of granting a magnetic pole position error  $X$

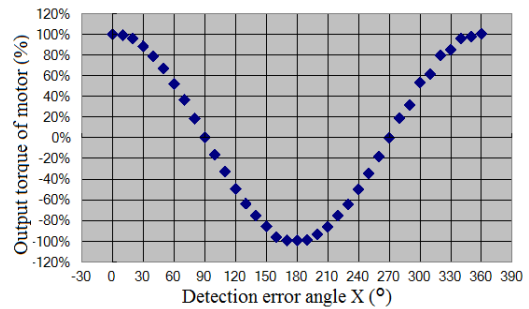


Fig. 10. Relationship between output torque of the motor and detection error angle  $X$

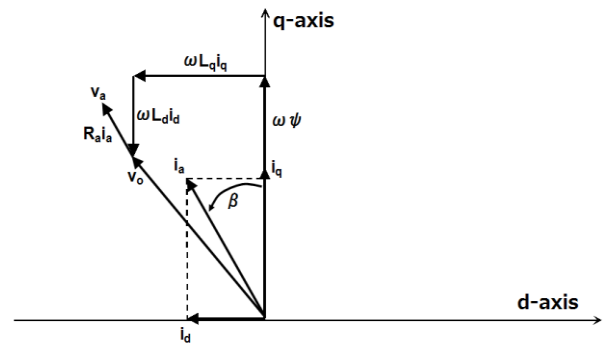
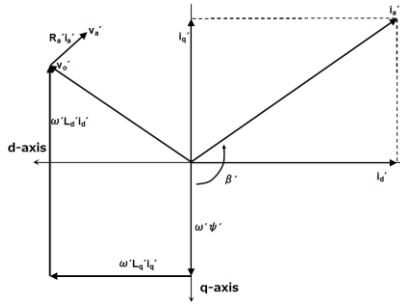


Fig. 11. Vector plot of PMSM



**Fig. 12.** Vector plot of PMSM in which there is the difference in magnetic pole position of 180 degrees in the case of Fig.11

Simultaneous s of dq-axis coordinate system of the PMSM is given by

$$\begin{bmatrix} V_d \\ V_q \end{bmatrix} = \begin{bmatrix} R_a + pL_d & -\omega L_q \\ \omega L_d & R_a + pL_q \end{bmatrix} \begin{bmatrix} i_d \\ i_q \end{bmatrix} + \begin{bmatrix} 0 \\ \omega\psi \end{bmatrix} \quad (9)$$

In (9),  $\psi$  is the effective value of the armature flux linkage by the permanent magnet,  $\omega$  is the angular velocity electricity,  $R_a$  is the armature winding resistance,  $p$  is the differential operator,  $V_d$  and  $V_q$  are dq-axis components of the armature voltage,  $i_d$  and  $i_q$  are dq-axis components of the armature current, and  $L_d$  and  $L_q$  are dq axis inductances.

Figs. 11 and 12 show each vector plot of PMSM that has a difference in the magnetic pole position of 180 degrees. In Figs. 11 and 12, vector of the induced voltage  $\omega\psi$  differs with magnetic pole position. Therefore, the voltage applied ( $= V_o + V_a - \omega\psi$ ) is different at motors 1 and 2. Therefore, the current  $I_{a'}$  flowing through motor 2 and the current  $I_a$  flowing through motor 1 have different phases and amplitudes.

For d-axis and q-axis current,  $I_{q'}$  is a negative value whereas  $I_q$  is positive. Furthermore, both  $I_d$  and  $I_{d'}$  are negative values, but they have different values. It is considered that since both directions of the d and q axes of two motors may be changed by the magnetic pole position, the value of d-axis and q-axis current flowing to motor 2 and the d-axis and q-axis current flowing to motor 1 become different values.

#### 4. Control Algorithm

The method to control two PMSMs that have different magnetic pole position using one inverter is considered by using the vector plot. The differences in torque and current of two motors are caused by the difference in magnetic pole position. Therefore, the control method is proposed by adjusting the position of magnetic poles, and next the vector control is performed for motor 1. The voltages injected into motors 1 and 2 by the inverter are the same. Therefore,  $I_d$

and  $I_q$  of the controlled motor can be controlled by using a current sensing value of the controlled motor. Therefore, this method mainly controls motor 1 by using its current value.

It is considered that to adjust the magnetic pole position, motors 1 and 2 should be rotated separately so that the magnetic pole position approaches the others. The difference in the magnetic pole position of two motors is in the range of  $-180 < (\theta_2 - \theta_1) \leq 180$ . In the range of  $-180 < (\theta_2 - \theta_1) < 0$ ,  $\theta_2$  is more delayed than  $\theta_1$ . Therefore, the magnetic pole position can be adjusted by rotating motor 1 in reverse and motor 2 forward. Also, in the range of  $180 \geq (\theta_2 - \theta_1) > 0$ ,  $\theta_2$  advances more than  $\theta_1$ .

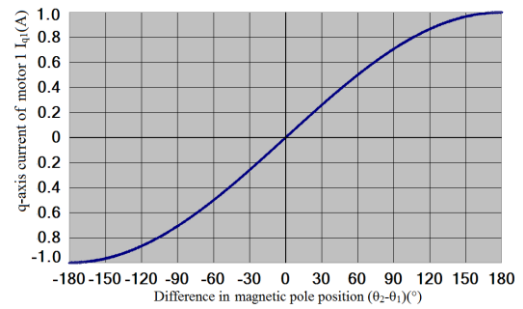


**Fig. 13.** Relationship between q-axis current of motor 1  $I_{q1}(A)$  and difference in magnetic pole position  $(\theta_2 - \theta_1)(^\circ)$

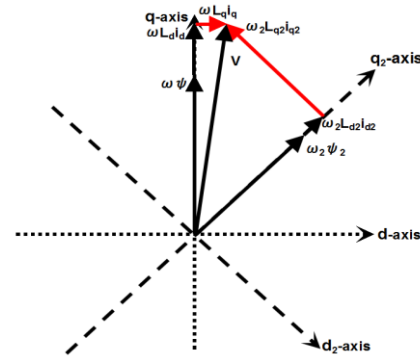


**Fig. 14.** Vector diagram that is plotted by (11) when proposed control method is performed in the range of  $-180 < (\theta_2 - \theta_1) < 0$

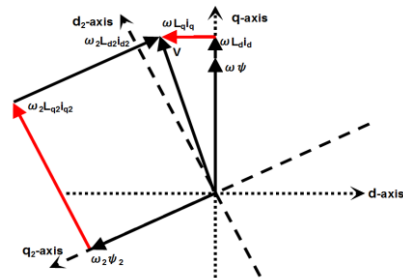


**Fig. 15.** Vector diagram plotted by (11) when control is performed to be proposed in the range of  $180 \geq (\theta_2 - \theta_1) > 0$

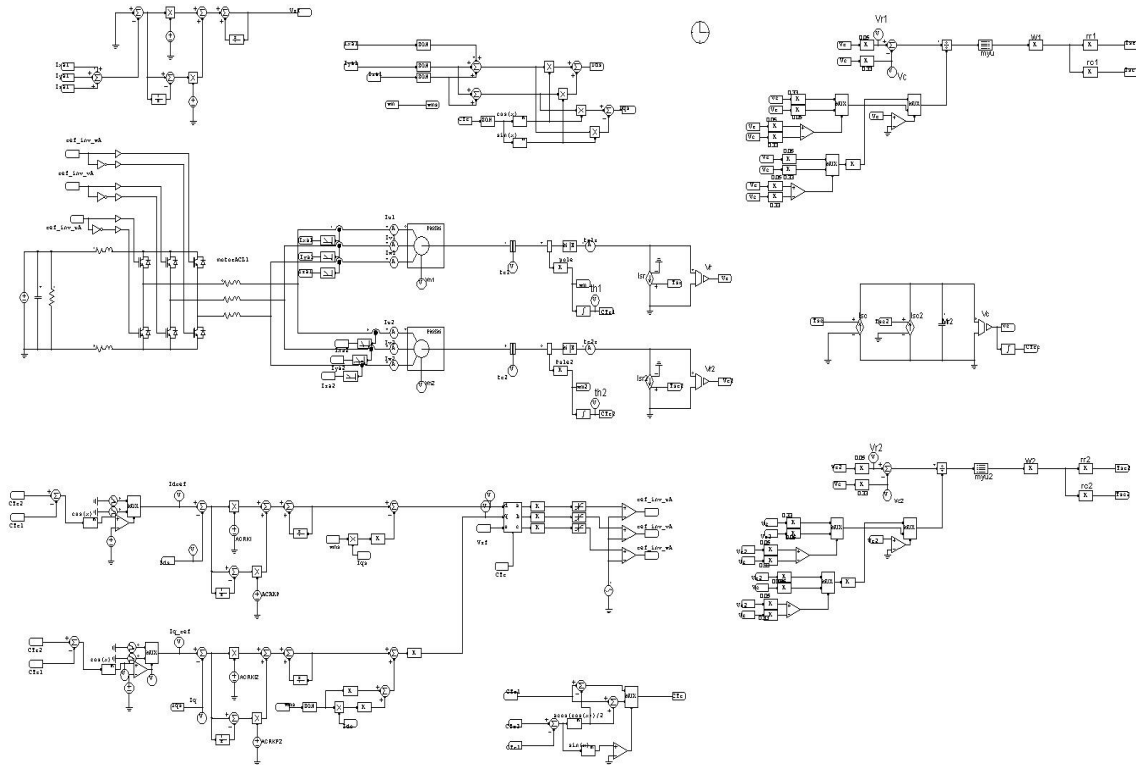


Fig. 16. Overall view of circuit on simulator (PSM)

Therefore, the magnetic pole position can be adjusted by rotating motor 1 forward and motor 2 in reverse. For  $I_q$  (q-axis current of the motor), by controlling the value of the negative  $I_q$ , the motor can be rotated in reverse. Additionally, by controlling the value of the positive  $I_q$ , the motor can be rotated forward. The direction of rotation is controlled by controlling  $I_q$ . Furthermore, it is considered that the position of the magnetic pole might be able to be adjusted faster by controlling  $I_{q1}$  to a bigger value as the difference of the magnetic pole position becomes larger. Therefore,  $I_{q1}$  is controlled to a bigger value as the difference in the magnetic pole position becomes larger.

The control method is described above. This method mainly controls motor 1 by using its current value. The magnetic pole position detection  $\theta'$  to be used in the control is calculated as  $\theta' = \theta_1 + (\theta_2 - \theta_1) / 2$  in this method. When  $\theta_1$  is different from  $\theta_2$  ( $\cos(\theta_2 - \theta_1) < 0.999$ ), to adjust the magnetic pole position of two motors by a large torque currents as soon as possible, d-axis and q-axis current command value is controlled to  $I_{d1} = \text{constant(A)}$   $I_{q1} = 0(\text{A})$ . When  $\theta_1$  and  $\theta_2$  are adjusted ( $\cos(\theta_2 - \theta_1) \geq 0.999$ ), d-q-axis current command values are controlled to  $I_{d1} = 0(\text{A})$   $I_{q1} = \text{constant(A)}$ . The methods used are called "the proposed control method" and "the magnetic pole position adjustment control method". To explain the logic of the position adjustment that is performed by this control method. When the detection pole position  $\theta'$  is  $\{\theta_1 + (\theta_2 - \theta_1) / 2\}$ ,  $I_q$  is 0,

and  $I_d$  is 1, torque component of motor 1  $I_{q1}$  is calculated by

$$I_{q1} = \sin\{(\theta_2 - \theta_1) / 2\} \tag{10}$$

In (10), Fig. 13 shows the relationship between q-axis current of motor 1  $I_{q1}(\text{A})$  and the difference in the magnetic pole position  $(\theta_2 - \theta_1)(^\circ)$  in a graph. From Fig.13, it is possible to output a large torque current  $I_{q1}$  as the difference in the magnetic pole position is large.

In the range  $-180 < (\theta_2 - \theta_1) < 0$ , negative torque current is output. In the range  $180 \geq (\theta_2 - \theta_1) > 0$ , positive torque current is output. Therefore, it is considered that control can be performed to adjust the magnetic pole position as described above by the proposed method. Because voltage  $V_a$  applied to the armature winding resistance  $R_a$  is a small value,  $V_o$  of motors 2 and motor 1 are assumed to be a similar value. Furthermore, motors is assumed to be a steady state. In this case, simultaneous s of dq-axis coordinate system of the PMSM are given by

$$\begin{bmatrix} V_d \\ V_q \end{bmatrix} = \begin{bmatrix} R_a + pL_d & -\omega L_q \\ \omega L_d & R_a + pL_q \end{bmatrix} \begin{bmatrix} i_d \\ i_q \end{bmatrix} + \begin{bmatrix} 0 \\ \omega\psi \end{bmatrix} \tag{11}$$

Fig. 14 shows the vector diagram that is plotted by (11) in the case of the performance of a control to be proposed in the range of  $-180 < (\theta_2 - \theta_1) < 0$ .  $I_d$  and  $I_q$  of motor 2 are determined by the difference in the induced voltage of motor 2  $\omega\psi$  and  $V_o$ . Because  $I_d$  and  $I_q$  are controlled to  $I_{d1} > 0$  and

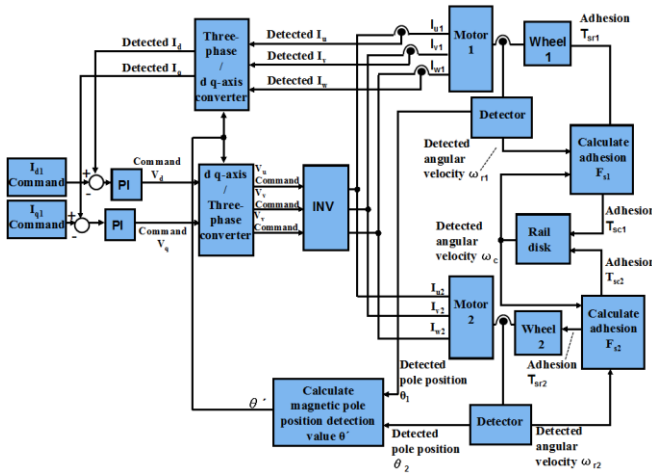


Fig. 17. Overall structure of proposed method

$I_{q1} < 0$ ,  $I_{q2}$  of motor 2 is positive from Fig. 14 in this range. Therefore, motor 1 rotates in reverse, and motor 2 rotates forward.

Fig. 15 shows the vector diagram that is plotted by (11) when the proposed control method is performed in the range of  $180 \geq (\theta_2 - \theta_1) > 0$ . Because  $I_d$  and  $I_q$  are controlled to  $I_d > 0$  and  $I_q > 0$ , in this range,  $I_{q2}$  of motor 2 is negative from Fig. 15. Therefore, motor 1 rotates forward, and motor 2 rotates in reverse.

After adjustment, for  $\theta_1 = \theta_2$ , the magnetic pole position detection value becomes  $\theta' = \theta_1 + (\theta_2 - \theta_1) / 2 = \theta_1 = \theta_2$ .

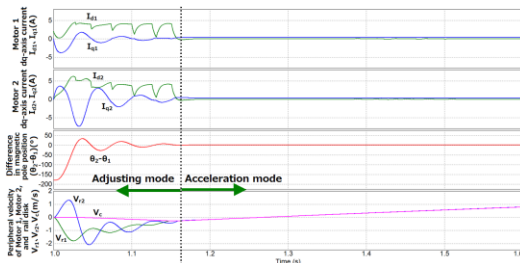


Fig. 18. Results in the case of  $(\theta_2 - \theta_1 = 180(\text{°}))$

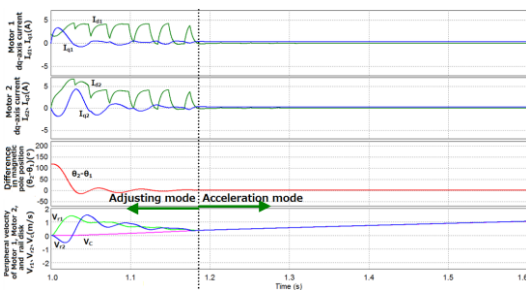


Fig. 19. Results in the case of  $(\theta_2 - \theta_1 = 120(\text{°}))$

From this, it is considered that by controlling  $I_{q1} = 1$  and  $I_{d1} = 0$ , q-axis current of motors 1 and 2 will be  $I_{q1} = I_{q2} = 1$ , and d-axis current of motors 1 and 2 will be  $I_{d1} = I_{d2} = 0$ ,

and motors 1 and 2 will be similarly rotated. Fig. 16 shows the overall view of the circuit on the simulator (PSIM). Fig. 17 shows the overall structure of the proposed method.

One inverter controls two PMSMs. Control of the motor is vector control using the current value of motor 1 and the magnetic pole position detection value  $\theta'$ .

### 5. Simulation Results

Figs. 18, 19, and 20 show graphs of the results of simulation of dq-axis current of motors 1 and 2,  $I_{d1}$  (A),  $I_{q1}$  (A),  $I_{d2}$  (A),  $I_{q2}$  (A), pole position of motor 1 and 2,  $\theta_1$  ( $^\circ$ ),  $\theta_2$  ( $^\circ$ ), difference in the magnetic pole position  $\theta_2 - \theta_1$  ( $^\circ$ ), peripheral velocity of the wheel of motors 1 and 2  $V_{r1}$  (m/s),  $V_{r2}$  (m/s), and peripheral velocity  $V_c$  of the rail disk (m/s). Fig. 18 shows the results when the difference in the initial magnetic pole position of  $\theta_1$  and  $\theta_2$  is 180 degrees. Fig. 19 shows the results when the difference in the initial magnetic pole position of  $\theta_1$  and  $\theta_2$  is 120 degrees. Fig. 20 shows the results when the difference in the initial magnetic pole position of  $\theta_1$  and  $\theta_2$  is -120 degrees. Since the control is performed to shift the pole position until  $t = 1$ (s), the figures show results for after  $t = 1$ (s).

From Figs. 18, 19, and 20,  $I_{q1}$  is positive when  $(\theta_2 - \theta_1)$  is positive,  $I_{q1}$  is also negative when  $(\theta_2 - \theta_1)$  is negative, and  $I_{q1}$  is greater when the value of  $(\theta_2 - \theta_1)$  is larger. That is,  $I_{q1}$  has a value nearly proportional to the difference in the magnetic pole position  $(\theta_2 - \theta_1)$ .

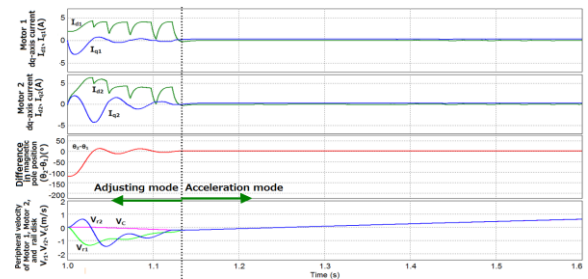


Fig. 20. Results in the case of  $(\theta_2 - \theta_1 = -120(\text{°}))$

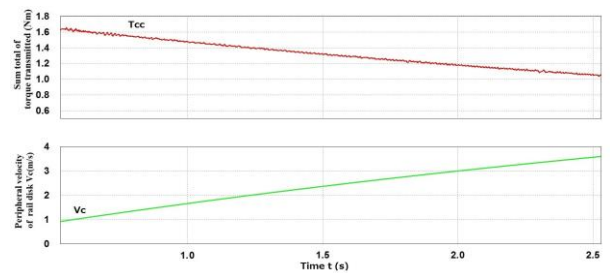


Fig. 21. Results for individual control in two inverters



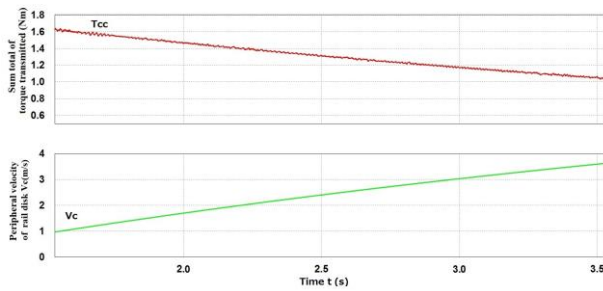


Fig. 22. Results of proposed control method

Also, for  $I_{q2}$ , when the difference in the magnetic pole position is large enough,  $I_{q2}$  moves to the opposite sign of  $I_{q1}$ . It is thought that this behavior is caused by the proposed control method and  $I_{q1}$  and  $I_{q2}$  were operated as proposed. From Figs. 18, 19, and 20, motor 2 and motor 1 are put into a state of idling slip by large  $I_q$  flows. Thus, magnetic pole positions can be adjusted in states in which the rail wheel is little affected. It is found that motor 2 and motor 1 rotate in different directions of the magnetic pole position in a state of idling slip. The magnetic pole position of the motor and circumferential speed of the wheel appear to vibrate. This is because the magnetic pole position of the two motors was adjusted abruptly from different locations. Therefore, it is considered that magnetic pole positions of the two motors would pass each other because there is no torque to act as a brake in the reverse direction. After the two magnetic pole positions pass each other, torque is applied to both in the opposite direction in order to make them match. Thus, both magnetic pole positions appear to vibrate. Since the difference in the magnetic pole position ( $\theta_2 - \theta_1$ ) becomes 0 at  $t \approx 1.2$  (s), it turns out that the magnetic pole positions can be adjusted.

## 6. Comparison with Individual Control

After magnetic pole positions were adjusted, the proposed control method and the individual control in two inverters were compared in terms of the sum total of the torque transmitted from two wheels to a disk by adhesion. Fig. 21 shows the results of the individual control in two inverters. Fig. 22 shows the results of the proposed control method. From Figs. 21 and 22, both methods transmitted the same adhesion torque. Therefore, two sets of PMSM can be controlled by one inverter in the proposed control methods.

## 7. Conclusion

This paper proposes a control method for two or more PMSMs using a one inverter. In the simulation results, two

sets of PMSM were able to be controlled by using one inverter.

## Acknowledgements

The authors thank everyone in the Electronics Circuit Laboratory, Department of Electronic Systems Engineering, School of Engineering, the University of Shiga Prefecture.

## References

- [1] H.B. Pacejka, E. Bakker: "The Magic Formula Tyre Model", Tyre models for vehicle dynamic analysis: proceedings of the 1st International Colloquium on Tyre Models for Vehicle Dynamics Analysis, held in Delft, The Netherlands (1991).



**Takuma Ito** received the B.S. degree of electronic systems engineering from The University of Shiga Prefecture in 2013. Since the same year, he has enrolled a master's course Graduate school of Engineering in The University of Shiga Prefecture. His research interest is an

inverter and a multi motors drive.



**Hiromi Inaba** was born in Tokyo, Japan, on September 1, 1950. He received the B.S. and Dr. Eng. degrees from Hokkaido University, Hokkaido, Japan, in 1974 and 1997, respectively. In 1974 he joined Hitachi Research Laboratory, Hitachi, Ltd., Ibaraki, Japan. He has been engaged in

research and development on an elevator and steel control system. In 2008, he became a Professor with the school of engineering, The University of Shiga prefecture, Shiga, Japan. Dr. Inaba is a member of the IEEE Industry Applications Society (IAS) and the Institute of Electrical Engineers (IEE) of Japan.



**Keiji Kishine** was born in Kyoto, Japan, on October 26, 1964. He received the B.S., and M.S. degrees in engineering science from Kyoto University, Kyoto, Japan, and Ph.D. degree from in informatics from Kyoto University, Kyoto, Japan, in 1990, 1992, and 2006, respectively. In 1992, he joined the

Electrical Communication Laboratories, Nippon Telegraph and Telephone Corporation (NTT), Tokyo, Japan. He has been engaged in research and design of high-speed, low-power circuits for Gbit/s LSIs using Si-bipolar transistors, with application to optical communication systems in NTT System

Electronics Laboratories, Kanagawa, Japan. From 1997, he has been worked on research and development of over Gbit/s Clock and Data Recovery IC at Network Service Innovation Laboratory in NTT Network Innovation Laboratories, Kanagawa, Japan. Now, He is working at Ubiquitous Interface Laboratory in NTT Microsystems Integration Laboratories, Kanagawa, Japan. In 2008, he became an Associate Professor with the school of engineering, The University of Shiga prefecture, Shiga, Japan. Dr. Kishine is a member of the IEEE Solid-State Circuits Society (SSCS) and Circuits and Systems (CAS), the Institute of Electronics, Information and Communication Engineers (IEICE) of Japan, the Institute of Electrical Engineers (IEE) of Japan.



**Mitsuki Nakai** received the B.S. and M.S. degrees of electronic systems engineering from The University of Shiga Prefecture in 2012 and 2014. In 2014, he joined Ishida Co., Ltd., Shiga, Japan. His research interest is a parallel connected power converter and motor drive.



**Keisuke Ishikura** received the B.S. degree of electronic systems engineering from The University of Shiga Prefecture in 2013. Since the same year, he has enrolled a master's course Graduate school of Engineering in The University of Shiga Prefecture. His research interest is a parallel connected power converter and motor drive.